PNAS RESEARCH ARTICLE | EARTH, ATMOSPHERIC, AND PLANETARY SCIENCES

Carbon mineralization with concurrent critical metal recovery from olivine

Fei Wang[a,1] and David Dreisinger[a]

Edited by Peter Kelemen, Lamont-Doherty Earth Observatory, Palisades, NY; received March 5, 2022; accepted June 26, 2022

Carbon dioxide utilization for enhanced metal recovery (EMR) during mineralization has been recently developed as part of CCUS (carbon capture, utilization, and storage). This paper describes fundamental studies on integrating CO_2 mineralization and concurrent selective metal extraction from natural olivine. Nearly 90% of nickel and cobalt extraction and mineral carbonation efficiency are achieved in a highly selective, single-step process. Direct aqueous mineral carbonation releases Ni^{2+} and Co^{2+} into aqueous solution for subsequent recovery, while Mg^{2+} and Fe^{2+} simultaneously convert to stable mineral carbonates for permanent CO_2 storage. This integrated process can be completed in neutral aqueous solution. Introduction of a metal-complexing ligand during mineral carbonation aids the highly selective extraction of Ni and Co over Fe and Mg. The ligand must have higher stability for Ni-/Co- complex ions compared with the Fe(II)-/Mg- complex ions and divalent metal carbonates. This single-step process with a suitable metal-complexing ligand is robust and utilizes carbonation processes under various kinetic regimes. This fundamental study provides a framework for further development and successful application of direct aqueous mineral carbonation with concurrent EMR. The enhanced metal extraction and CO_2 mineralization process may have implications for the clean energy transition, CO_2 storage and utilization, and development of new critical metal resources.

carbon mineralization | concurrently enhanced metal recovery (cEMR) | global warming mitigation | mineral carbonation | clean energy transition

Significance

Global warming mitigation and energy transition require effective CO_2 emission reduction and enhanced supply of critical metals. Carbon mineralization and concurrent critical metal recovery using a metal-complexing ligand offer a significant opportunity to simultaneously achieve both objectives for sustainable development. The utilization of ex situ direct aqueous mineral carbonation can potentially make the CO_2 mineralization process economically feasible owing to the value of nickel and cobalt recovered and comprehensive usage of mineral resources to sequester carbon and realize carbon credits. The success of high carbon mineralization efficiency and highly selective metal extraction in one step makes the accelerated mineral carbonation applicable. Nickel recovery from olivine silicate minerals can increase global metal production and expand the reserves of explorable nickel resources.

Carbon capture, utilization, and storage (CCUS) (1–5) has attracted worldwide attention to mitigate global warming effectively and reduce capital costs of CO_2 sequestration. Accelerated mineral carbonation has been considered as a promising method in terms of CCUS to control excessive CO_2 emissions (6–12) owing to advantages of fast reaction kinetics and stable mineral carbonate products (13–15). However, the high capital and operating cost of accelerated mineral carbonation limits its application due to the requirements of elevated temperature and pressure for ex-situ direct aqueous mineral carbonation (14, 16) and consumption of chemical reagents and energy for ex-situ indirect aqueous mineral carbonation (17–19). Enormous efforts have been made to compensate for the capital cost with utilization for other technologies (20–25) such as electricity generation (21), hydrogen generation (22), and producing the construction materials (23) nano silica (24) and pure magnesium carbonate (25). It is noted that feedstock for mineral carbonation usually comes from minerals engineering (mining and mineral processing) and also contains valuable metals (1, 3, 15, 26, 27). Since 2017, the concept that CO_2 sequestration is utilized for enhanced metal recovery (EMR) has been officially introduced (1, 3, 26, 27). During CO_2 sequestration, metals may be leached into solution with the dissolution of feedstock, while CO_2 can be stabilized into mineral carbonates. The profits from recovered valuable metals, e.g., nickel and cobalt, can potentially outweigh the costs of carbon mineralization and render ex-situ treatment economically attractive. The operational cost for mineral carbonation applied to olivine has been estimated at ~$68 to $112/t sequestered CO_2 based on O'Connor et al. (28) and Huijgen et al. (29), with a ~3 to 5% annual inflation rate. If all nickel in the olivine (0.27% nickel content, 0.55 t CO_2/t olivine of theoretical mineral carbonation capacity) (30) can be recovered through the accelerated mineral carbonation, the recovered nickel value can potentially reach $162/t sequestered CO_2 (requires 1.8 t olivine) at the current nickel price $33,144/t nickel (Trading Economics (31)). The potential value of the recovered nickel is higher than the cost. This is not only important for global warming mitigation but also significant to achieve sustainable resource utilization.

However, there are only a few reports (27, 32, 33) on carbon mineralization with EMR thus far, and these reports mainly focus on ex-situ indirect mineral carbonation, i.e., pH-swing process. Kashefi et al. (32) used hydrochloric acid to leach alkaline red

Author affiliations: [a]Department of Materials Engineering, The University of British Columbia, Vancouver, BC V6T 1Z4, Canada

Author contributions: F.W. designed research; F.W. performed research; F.W. and D.D. analyzed data; F.W. wrote the paper; D.D. supervised the study; and D.D. edited the paper.

The authors declare no competing interest.

This article is a PNAS Direct Submission.

[1]To whom correspondence may be addressed. Email: fei.wang@alumni.ubc.ca.

This article contains supporting information online at http://www.pnas.org/lookup/suppl/doi:10.1073/pnas.2203937119/-/DCSupplemental.

Published August 1, 2022.

mud to enrich ferric oxide for further reuse and to extract aluminum and calcium in solution, which can be precipitated sequentially by consumption of sodium hydroxide and sodium bicarbonate, respectively. The consumption of hydrochloric acid and sodium hydroxide may make this process unattractive. Hamilton et al. (27) also used diluted sulfuric acid to heap leach ultramafic mine tailings to release trace metals, followed by precipitation as mineral carbonates and hydroxides with 10% CO_2 gas. The consumption of acid and slow kinetics may make the process economically unfavorable. Zappala et al. (33) utilized the dissolution of olivine from a laterite in sulfuric acid and the gradual increase in pH value by gradually adding triethylamine to precipitate impurities of iron and aluminum and recover nickel as a precipitate, followed by carbonation precipitation of magnesium with supply of a combustion flue gas and heating of the solution to 100 °C to evaporate and recycle triethylamine. The saprolite ore containing 1.28% nickel was treated as a waste laterite, and olivine was the dominant reactive mineral, whereas lizardite was almost left unreacted. Although it is an important progress for utilization of CO_2 mineralization, there are significant improvements required for application, e.g., the slow kinetics (more than 40 h), low nickel recovery (~70%), and a complex multiple-steps operation.

Ex-situ direct aqueous mineral carbonation might be preferred because of the fast kinetics and simplicity (13–15). However, there is only one report (30) on ex-situ direct aqueous mineral carbonation with EMR thus far. Our previous study (30) confirms that direct aqueous mineral carbonation of olivine can be utilized for concurrent nickel conversion from nickel silicate to nickel sulfide for subsequent recovery. This process is based on the higher stability of nickel sulfide than iron sulfide and metal carbonates. With supply of a CO_2-H_2S gas mixture, magnesium and ferrous iron from olivine sequestered CO_2 to form stable mineral carbonates, and meanwhile, nickel from the olivine crystal structure formed nickel sulfide particles on the surface of precipitated carbonates. This process applied the fundamental mechanism of mineral carbonation of olivine that the olivine is dissolved by protons and (bi)carbonate ions and releases divalent metal ions into aqueous solution followed by precipitation as mineral carbonates (34). Although this is also an important development for CO_2 utilization, the use of hazardous H_2S, significant coprecipitation of ferrous iron sulfide with the nickel sulfide, and kinetic competition in precipitation of carbonates and sulfides result in limited prospects for commercial application. In fact, ex-situ mineral carbonation has significant potential to enhance CO_2 storage of captured CO_2 from combustion flue gases or direct air capture (35, 36). The production of alkaline wastes that can be important feedstocks for ex-situ direct aqueous mineral carbonation and valuable metals recovery are increasing (37). The clean energy transition requires significantly enhanced supply of critical metals, including nickel and cobalt (38). It is therefore still urgently required to develop a green and sustainable mineral carbonation process with EMR.

Our previous research (39) has confirmed that carbonation of olivine is the dominant reaction of impure natural silicate samples at elevated CO_2 partial pressure (pCO_2) and temperature. Other minerals including serpentine and pyroxene are difficult to react. Therefore, the further development on ex-situ CO_2 mineralization used a natural olivine sample containing nickel and cobalt in this research. In this work, a metal-complexing ligand was used to selectively complex and extract nickel and cobalt into aqueous solution during carbonation. To prevent nickel and cobalt ions from precipitating as carbonate minerals, the stability of the nickel- and cobalt- complex ions must be greater than that of the corresponding carbonates. Disodium ethylenediaminetetraacetate (EDTA) was used in this work as an example. This study describes the development of ex-situ direct aqueous mineral carbonation to concurrently achieve highly selective extraction of nickel and cobalt from the olivine crystal structure in one step via addition of a metal-complexing ligand.

Results and Discussion

Importance of Complex Ligand for Simultaneous EMR During Carbon Mineralization. Carbon mineralization was undertaken at a temperature of 155 °C and a pCO_2 of 34.5 bar with a solution of 1.5 molal sodium bicarbonate (40). Sodium bicarbonate facilitates transfer of CO_2 from the gas phase to mineral carbonate precipitates, enhances the diffusion of aqueous silica to accelerate mineral carbonation (34), and forms a buffered system with carbonic acid in solution to regulate pH for mineral carbonate precipitation. The only difference between direct aqueous mineral carbonation and concurrent utilization (i.e., mineral carbonation and simultaneous EMR in a single step) is the addition of the metal-complexing ligand. A suitable ligand must be chosen to recover valuable nickel and cobalt effectively. EDTA was studied in comparison with two other common ligands, citrate (41, 42) and glycine (43), as shown in Fig. 1. All ligands were prepared as 0.1 molal sodium salt solution and added prior to carbon mineralization. However, no nickel recovery from carbon mineralization was evident with citrate and glycine addition, although the extent of olivine carbonation increased with time. Citrate and glycine are therefore not suitable for carbon mineralization and concurrent metal recovery. Citrate and glycine were ineffective due to the lower stability of the metal-complex ions compared with the corresponding metal carbonates. The log stability constant of nickel- citrate and glycine complex ions is around 5.4 (44, 45) and 6.1 (46), respectively (for the 1:1 complexes), which is far smaller than the log stability constant (11.0) of nickel carbonate. Cobalt behaves similarly to nickel. As a result, the released Ni^{2+} and Co^{2+} from the olivine crystal structure directly coprecipitated as mineral carbonates together with Mg- and Fe- carbonates. In contrast, metal-EDTA complex ions are more stable than the corresponding metal carbonates, and Ni- and Co- EDTA

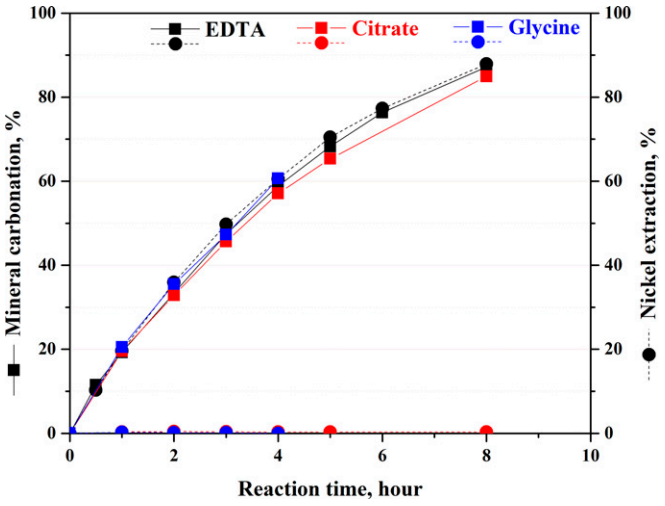

Fig. 1. Types of complex ligand to test suitability for mineral carbonation with concurrently selective metal extraction at 155 °C, pCO_2 = 34.5 bar, and 1.5 m $NaHCO_3$: EDTA (black); citrate (red), and glycine (blue).

complexes are stronger than the other divalent metal-complex ions, as shown in *SI Appendix*, Table S1. With using EDTA, the nickel extraction efficiency matched the mineral carbonation efficiency throughout the reaction time. EDTA was a suitable ligand as expected. Other EDTA-group ligands can also potentially work for this EMR system, including glycoletherdiamine-N,N,N′,N′-tetraacetic acid and 1,2-cyclohexylenedinitrilotetraacetic acid (47). Therefore, ligand selection for carbon mineralization and concurrent metal extraction should meet the following requirements: a) metal-complex ions with ligands must be more stable than the corresponding metal carbonates, and b) complex ions of nickel and cobalt with ligands are more stable than corresponding complex ions of iron and magnesium. EDTA, as an example of a suitable ligand, is inexpensive and may be recycled (48) throughout the carbon mineralization and metal recovery processes.

Selectivity of Metal Recovery during Carbon Mineralization. As shown in *SI Appendix*, Table S1, the Ni-EDTA and Co-EDTA complex ions are more stable than $NiCO_3$ and $CoCO_3$. With mineral carbonation, Ni^{2+} and Co^{2+} released from the olivine crystal structure preferred to form more stable Ni-EDTA and Co-EDTA complex ions in aqueous solution rather than to precipitate as mineral carbonates. Meanwhile, it is also important to note that the stability of Ni-EDTA and Co-EDTA is also greater than that of Fe-EDTA, Mg-EDTA, and Ca-EDTA, so that Ni-EDTA and Co-EDTA formed preferentially. In contrast, Fe^{2+} and Mg^{2+} (and Ca^{2+}, if present) ions from dissolved olivine can precipitate as stable mineral carbonates under limited amounts of EDTA in solution. The selectivity of metal recovery during mineral carbonation was tested with control of the EDTA dosage. For the direct aqueous carbonation system, the pH value is around 7.2 at 1.5 molal sodium bicarbonate and pCO_2 = 34.5 bar (34). Thus, the dominant species of free EDTA and divalent metal (Me)-EDTA complex are expected to be $[HEDTA]^{3-}$ and $[Me\text{-}EDTA]^{2-}$ in aqueous solution, respectively (49). The theoretical requirement for EDTA dosage is an EDTA/TNi (total Ni) molar ratio of 1.0. As shown in Fig. 2*A*, without addition of EDTA, there was no metal recovery in aqueous solution, and all divalent metals from the olivine crystal structure were precipitated as mineral carbonates with a mineral carbonation efficiency of 87% at 8 h. With a gradual increase of EDTA amount, Ni extraction was the first to increase and reached the same value as the mineral carbonation efficiency at 1.21 molar ratio of EDTA/TNi. The Ni extraction efficiency was virtually the same as the mineral carbonation efficiency because both are measures of reaction progress, and all divalent metals should be essentially homogeneously distributed in pure olivine. Further increase of EDTA dosage did not increase Ni recovery since all released Ni ions via mineral carbonation have been extracted. The change in Ni recovery can be seen from the change in concentration of aqueous $[Ni(EDTA)]^{2-}$ complex ions, as shown in Fig. 2*B*. Similar to Ni, Co recovery also increased markedly with the increasing dosage of EDTA and reached the same value as the mineral carbonation efficiency. The concentration of aqueous $[Co(EDTA)]^{2-}$ complex ions showed the same trend to Co recovery as indicated in Fig. 2*C*, although the maximum value was 2.3 mg/L because of the low Co content (0.0055%) in raw olivine. It is also noted that the acceleration rate of increased Co recovery was smaller than that of nickel recovery. There was no Co recovery within 0.51 molar ratio of EDTA/TNi, whereas Ni recovery was 57%. Ni forms the strongest complex with EDTA, followed by Co, as shown in *SI Appendix*, Table S1. In contrast, only a very small amount of Fe was present in aqueous solution with increase in EDTA, at 0, 1.3%, 2.6%, and 5.7% Fe extraction for EDTA/TNi = 0.51, 1.0, 1.21, and 2.0, respectively. All Mg contributed to the formation of magnesite, and the Mg left in solution was negligible (<6 mg/L). Different from the slight increasing trend in Fe recovery, concentration of $[Fe(EDTA)]^{2-}$ complex ions in aqueous solution dramatically rose from ∼0–113 mg/L when the molar ratio of EDTA/TNi increased from 0.51 to 2.0, as shown in Fig. 2*D*. With further increase in EDTA dosage, it is very likely that Fe-EDTA would continue to increase. Because of the high Fe content (7.09%) of the raw olivine compared with the Ni and Co contents, the rapid increase did not clearly show in Fe recovery (Fig. 2*A*). Iron in solution is not desirable. The excessive Fe(II)-EDTA ions in aqueous solution may be oxidized by air to Fe(III)-EDTA complex ions, which are more stable than $[Ni(EDTA)]^{2-}$ and $[Co(EDTA)]^{2-}$, and thus may result in challenges during further processing procedures to produce final Ni and Co products from the solution. It is important to carefully control the EDTA dosage during mineral carbonation to reduce the amount of Fe ions in solution. The Mg concentration just slightly increased to below 6 mg/L with increasing EDTA/TNi molar ratio to 2.0, as shown in Fig. 2*E*. $[Mg(EDTA)]^{2-}$ complex ions are the least favored to form compared with other EDTA complex ions, including Fe(II)-EDTA. The priority of divalent metal-EDTA complex is $Ni^{2+}>Co^{2+}>Fe^{2+}>Mg^{2+}$. The highly selective metal extraction and concurrent aqueous mineral carbonation can be achieved in one step.

Complex Competition for Selective Metal Recovery and Concurrent Carbon Mineralization. Preloading ligand to the reaction system prior to mineral carbonation is suitable for potential application. Having acquired the experience on mineral carbonation

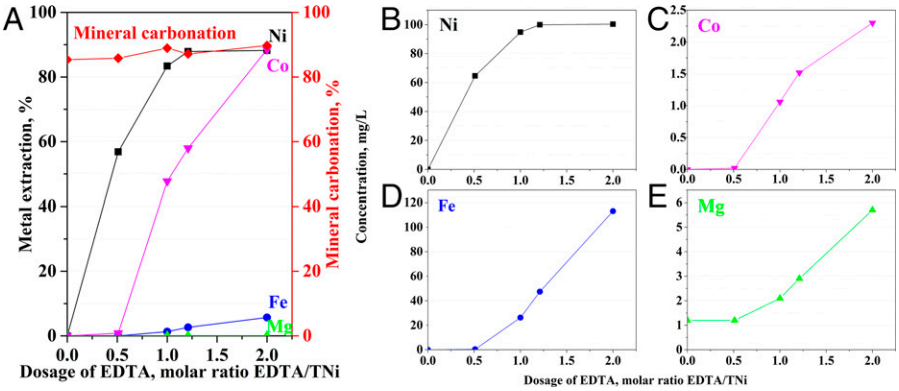

Fig. 2. Selectivity of metal recovery dependent on dosage of EDTA/TNi molar ratio at 155 °C, pCO_2 = 34.5 bar, and 1.5 m $NaHCO_3$ in 8 h: (*A*) metal recovery and mineral carbonation efficiency; (*B*) nickel concentration; (*C*) cobalt concentration; (*D*) iron concentration; and (*E*) magnesium concentration.

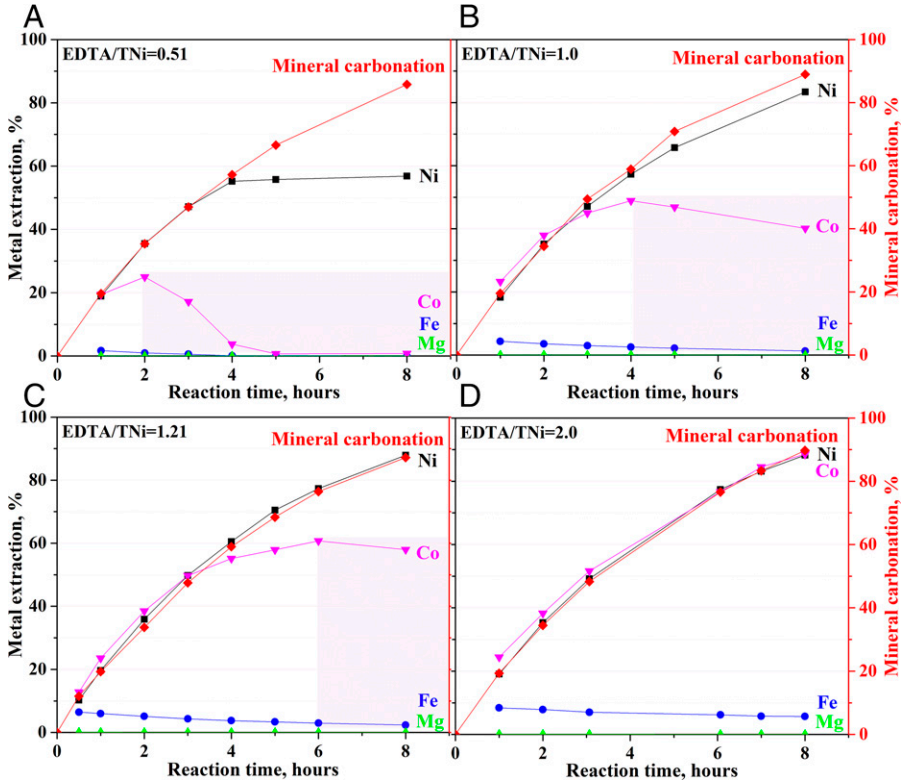

Fig. 3. Complex competition of divalent metals for selective metal recovery during mineral carbonation at various dosage of EDTA/TNi at 155 °C, pCO_2 = 34.5 bar, and 1.5 m $NaHCO_3$: (*A*) 0.51, (*B*) 1.0, (*C*) 1.21, and (*D*) 2.0.

and concurrent nickel sulfidization (30), preloading chemical reagents might result in decrease in selectivity of metal recovery. Therefore, metal extraction at each EDTA dosage was monitored in detail. When the EDTA dosage was far below the theoretical need for efficient metal recovery as shown in Fig. 3*A*, i.e., EDTA/TNi = 0.51, nickel recovery gradually increased to 55% together with mineral carbonation at 4 h of reaction time. After 4 h, no more nickel was recovered in aqueous solution, even though mineral carbonation efficiency continued to increase significantly. All EDTA ligand formed $[Ni(EDTA)]^{2-}$ complex ions at 4 h, and no further EDTA was available to chelate the continuously released Ni^{2+} from olivine owing to ongoing mineral carbonation. Due to the complex priority of EDTA, $Ni^{2+}>Co^{2+}>Fe^{2+}>Mg^{2+}$, cobalt recovery only increased to 25% at 2 h, followed by a decrease. The cobalt-EDTA complex is believed to release ligand for preferentially chelating Ni^{2+}. Iron extraction remained at a very low level, from 1.7% at 1 h decreasing to 0% after 4 h. Similarly, when EDTA was added at the theoretical dosage, EDTA/TNi = 1.0 (Fig. 3*B*), Ni recovery continued to increase throughout the carbonation process, although it was still slightly lower than the corresponding carbonation efficiency, 83% vs. 88%. The maximum Co recovery shifted from 25% at 2 h at EDTA/TNi = 0.51–49% at 4 h at EDTA/TNi = 1.0; Fe extraction also decreased from 4.3% at 1 h to only 1.3% at 8 h. The valuable metal extraction became better with a further slight increase in EDTA/TNi to 1.21 (Fig. 3*C*). Ni extraction efficiency remained the same as carbonation efficiency throughout the CO_2 sequestration process; Co recovery reached the maximum at 61% at 6 h, followed by a slight decrease; Fe extraction had a decreasing trend from 6.5% at 0.5 h to 2.4% at 8 h. The use of double the theoretical dosage of EDTA (Fig. 3*D*) did not further increase Ni recovery but increased Co recovery to match the carbon mineralization efficiency. In contrast, Fe recovery reached a higher level and decreased from 8.4% at 1 h to 5.7% at 8 h. All magnesium ions released from olivine carbonation precipitated as magnesium carbonate (magnesite). With the trend of increase in Ni recovery during CO_2 mineralization, Fe extraction exhibited a decreasing trend, which may be accompanied by a decreasing Co extraction at a reduced dosage of EDTA. There was a complex competition among divalent metal ions during carbon mineralization, as shown in the following reactions (Eqs. **1** to **3**). The released free metal ions during competition precipitated as mineral carbonates. An increase in ligand amount can alleviate the complex competition, especially between Ni and Co:

$$[Co(EDTA)]^{2-} + Ni^{2+} = [Ni(EDTA)]^{2-} + Co^{2+} \quad [1]$$

$$[Fe(EDTA)]^{2-} + Co^{2+} = [Co(EDTA)]^{2-} + Fe^{2+} \quad [2]$$

$$[Mg(EDTA)]^{2-} + Fe^{2+} = [Fe(EDTA)]^{2-} + Mg^{2+} \quad [3]$$

Suitability at Different Temperatures and CO_2 Pressures. Application of CO_2 mineralization and concurrent utilization may be challenged by many uncertainties, including energy requirements and CO_2 pressure supply. It is important for an innovative process to be robust at various temperatures and pCO_2. This carbon mineralization with EMR process was tested at 135 °C, 155 °C, and 175 °C as shown in Fig. 4*A* and at pCO_2 = 20.7 bar, 27.6 bar, and 34.5 bar as shown in Fig. 4*B*. The dosage of EDTA was maintained at EDTA/TNi = 1.2. Temperature in the range of 135 °C–175 °C does not affect the kinetic control regime of mineral carbonation based on previous research (34). At pCO_2 = 34.5 bar and 1.5 molal $NaHCO_3$, the mineral carbonation was kinetically controlled by dissolution of olivine (34). With addition of EDTA, all

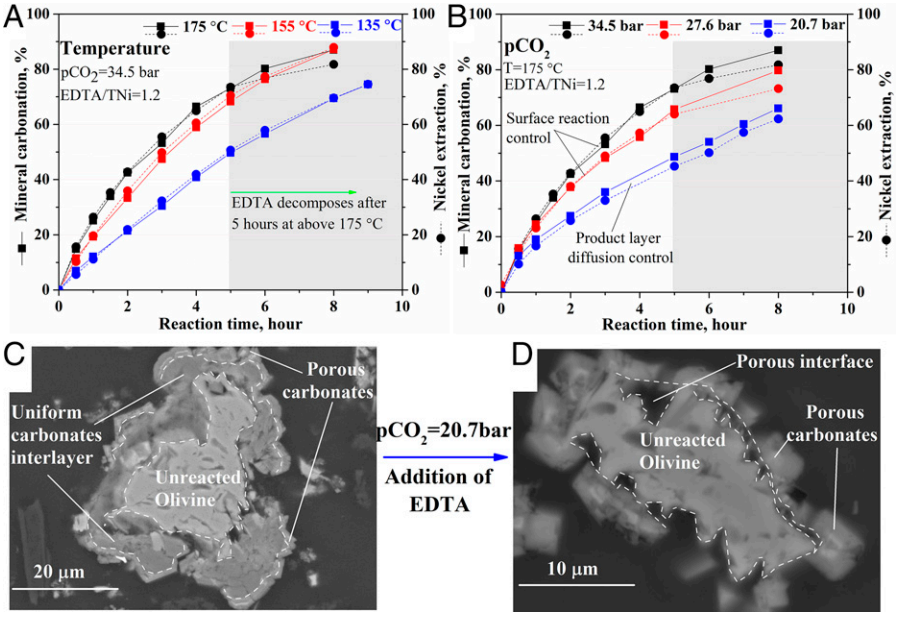

Fig. 4. Suitability of mineral carbonation and concurrent metal recovery at (*A*) various temperatures and (*B*) various pCO_2 and the positive effects of EDTA on kinetic regime of mineral carbonation varying from (*C*) uniform carbonate layer diffusion control without addition of EDTA to (*D*) surface reaction control with addition of EDTA.

released Ni was recovered in aqueous solution at all three temperatures. The results further confirm that mineral carbonation is required for concurrent nickel recovery. However, Ni recovery at 175 °C started to be inferior to the corresponding carbonation efficiency after 5 h, and the difference became obvious with time. In contrast, Ni recovery remained the same as the corresponding mineralization efficiency at both 155 °C and 135 °C. At 155 °C, the carbonation and Ni recovery in 8 h reached the same value as the carbonation efficiency at 175 °C. This contrast is postulated to be due to EDTA degradation at 175 °C or higher (50). In order to effectively recover Ni and Co and to enable recycling of EDTA, it is recommended to avoid operating at temperatures at or above 175 °C.

The change of pCO_2 can alter the kinetic control regime of mineral carbonation of olivine, even with addition of sodium bicarbonate (34, 40). The mineral carbonation of olivine was kinetically controlled by diffusion through a uniform carbonate layer at pCO_2 = 20.7 bar without addition of EDTA as shown in Fig. 4*C*, whereas the carbonation at pCO_2 = 27.6 bar and 34.5 bar was controlled by dissolution of olivine based on our previous study (34, 40). The suitability of this innovation was further tested under different kinetic control regimes at different pCO_2, as shown in Fig. 4*B*. Ni recovery kept increasing with mineral carbonation at all three pCO_2. Carbon mineralization and concurrent metal recovery were observed under both kinetic control regimes. Since the temperature was 175 °C, Ni recovery after 5 h began to be lower than corresponding carbonation efficiency at pCO_2 = 34.5 bar and 27.6 bar due to degradation of EDTA. However, the detrimental effect of EDTA degradation did not show at pCO_2 = 20.7 bar, although Ni recovery was less than 4% lower than the corresponding carbonation efficiency. The reason may be because the effective amount of EDTA remaining was still more than the required amount to chelate Ni^{2+}. The highest mineral carbonation and nickel recovery values at 8 h were below 66%, where the detrimental effect began to be shown at pCO_2 = 27.6 bar. In addition, the scanning electron microscope (SEM) images on cross-sections through reacted particles indicate another beneficial effect of EDTA as shown in Fig. 4*D* that is the characteristic texture of reacted olivine under surface reaction control (30, 34, 39, 40). The uniform carbonate layer between the unreacted olivine core and a porous carbonate layer (Fig. 4*C*) at pCO_2 = 20.7 bar (34) was not observed with addition of EDTA. In turn, a porous interlayer showed up in Fig. 4*D*. The corresponding SEM with energy dispersive X-ray detector data (*SI Appendix*, Fig. S1) can further confirm this variation of kinetic regime. The direct aqueous mineral carbonation process can be slightly accelerated by EDTA. This may be the reason why mineral carbonation efficiency slightly increased from 85% without EDTA to 90% at EDTA/TNi = 2.0 at 155 °C as shown in Fig. 1*A* and why the nickel recovery in 8 h at 155 °C reached the same value as at 175 °C, as shown in Fig. 4*A*. Addition of EDTA can not only effectively chelate valuable Ni^{2+} and Co^{2+} for recovery but can also accelerate the carbon mineralization process by shifting the kinetic regime from diffusion control to surface reaction control. It is therefore concluded that this CO_2 mineralization and concurrent utilization for EMR process is robust at various temperatures and pCO_2.

Conclusion: Carbon Mineralization and Highly Selective Metal Extraction. This work forms the basis for an innovative and robust process that integrates CO_2 mineralization and EMR from olivine. Nearly 90% nickel and cobalt extraction and mineral carbonation efficiency were simultaneously achieved in a highly selective single-step process. The optimized conditions were 155 °C, 34.5 bar of pCO_2, 1.5 molality sodium bicarbonate with an EDTA dosage of EDTA/TNi = ~1.2 to 2.0 and up to 8-h reaction. In this process, each t olivine can permanently stabilize 0.49 t CO_2 gas as mineral carbonates and simultaneously 1.97 kg (4.35 lb) nickel and 0.05 kg (0.11 lb) cobalt were extracted. The extracted aqueous nickel- and cobalt- EDTA complex in aqueous solution can be easily separated from the solid carbonates. The selective metal extraction and mineral carbonation can be conducted at various temperatures and kinetic control regimes. This innovation may have implications for the clean energy transition, enhanced CO_2 storage and utilization, and enhanced supply of critical metals.

Further optimization is needed for potential scale-up, including alternative ligands, increase in reaction rates, and the suitability of other mineral feedstocks.

Materials and Methods

Materials. A natural olivine sample provided by Sibelco Europe was used in this research. The chemical composition was analyzed by digestion and inductively coupled plasma atomic emission spectroscopy (ICP-AES), as shown in *SI Appendix*, Table S2. This high-grade olivine contains 0.22 wt% nickel and 0.0055 wt% cobalt in the olivine crystal structure. The mineral composition of the high-grade olivine based on quantitative X-ray diffraction analysis is shown in *SI Appendix*, Table S3. This natural olivine sample comprised 86.4 wt% olivine, 6.3 wt% enstatite, 1.4 wt% serpentine, and 5.9 wt% other silicate minerals. The composition of the sample is comparable to dunnite (39). The maximum mineral carbonation capacity is 0.55 t CO_2 per t of olivine sample, based on contents of total magnesium, iron, and calcium. The particle size was $P_{80} = 30$ μm with specific surface area 1.17 m^2/g through a rod-mill grinding. A fine size was selected to accelerate the kinetics of the carbonation and metal extraction processes.

EDTA solution with 0.1 molal Na_2EDTA concentration was prepared prior to mineral carbonation tests and worked as a complexing ligand. Sodium bicarbonate was also used at 1.5 molal based on previous mineral carbonation research (40, 51). A high-purity CO_2 compressed gas (>99.9%) was used as the CO_2 supply.

Methods. The direct aqueous mineral carbonation tests were carried out in a 600 mL stainless steel autoclave (No. 5103, Parr Instrument Company, USA) with a 12 mL sampling kit at temperatures between 135 °C and 175 °C and pCO_2 between 20.7 bar and 34.5 bar, as described in a previous study (34). EDTA solution at different dosages of EDTA/TNi (total nickel) molar ratio up to 2.0 was preloaded with 5 (wt/wt)% olivine slurry and 1.5 molal $NaHCO_3$ concentration for carbonation and metal extraction. During mineral carbonation, slurry samples were extracted at 30-min intervals for the first 2 h and every hour toward the end of the test, followed by a centrifuge system for solid/liquid separation. The liquid was further filtered through a 0.45 μm nylon membrane to obtain aqueous solution analysis for nickel, cobalt, iron, and magnesium via ICP-AES; the solid was washed twice with deionized water and then dried at 60 °C in an oven for total carbon analysis via LECO CS3200 instrument and mineral composition analysis via X-ray diffraction (XRD, Rigaku MultiFlex) and morphology analysis via SEM with an energy dispersive X-ray detector (SEM-EDX, FEI Quanta 650 instrument).

The methods to calculate the mineral carbonation efficiency are based on Eqs. **4** and **5** (34, 40). The difference in mineral carbonation efficiency based on the changes in mass (Eq. **4**) and the changes in carbon content is less than ±2% and the mineral carbonation efficiency presented in this work is reliable. The metal extraction efficiency is calculated based on Eq. **6**. The error of the metal extraction efficiency is estimated at ±2%, ±6%, ±0.2%, and ±0.05% for nickel, cobalt, iron, and magnesium, respectively. The difference in metal extraction for the metals is mainly due to the variations in the original content of the metals in the olivine sample:

$$\alpha = \frac{m_2 \times \theta_2 - m_1 \times \theta_1}{m \times m_1} \times \frac{44.0098}{12.011} \times 100\%, \quad [4]$$

$$\alpha = \frac{\theta_2 - \theta_1}{m \times (\frac{12.011}{44.0098} - \theta_2)} \times 100\%, \quad [5]$$

$$\beta_{Me} = \frac{C_{me} \times V}{m_1 \times \delta_{Me}} \times 100\%, \quad [6]$$

where, m_1 and m_2 represent the amounts of the raw material and the product solid after mineral carbonation, respectively, with units of t; m is the mineral carbonation capacity of the raw materials with unit of t CO_2/t material, which is only calculated based on the divalent metal content of the sample and is not related to the type of minerals or mineral compositions; θ_1 and θ_2 are the total carbon content in %, of the solid before and after carbonation, respectively; α is the mineral carbonation efficiency in %; β_{Me} is the metal extraction efficiency for each of the divalent metal (nickel, cobalt, iron, and magnesium) in %; δ_{Me} is the original content of each of the divalent metal content in the olivine sample shown in *SI Appendix*, Table S2; and C_{Me} is the concentration of each the divalent metal in aqueous solution after mineral carbonation in mg/L and V is the volume of the aqueous solution for the test in L.

Data Availability. All study data are included in the article and/or *SI Appendix*.

ACKNOWLEDGMENTS. We acknowledge Sibelco Europe for providing the olivine mineral sample. Mitacs Accelerate and LeadFX provided financial support for this fundamental research. We also thank Dr. Berend Wassink, Professor Edouard Asselin, Ms. Yuchang Xiao, and Ms. Maggie Chong for providing technical support.

1. T. Niass, S. Aramco, S. Arabia, J. Kislear, Mission Innovation, Accelerating the Clean Energy Revolution: Carbon Capture Innovation Challenge: Report of the Carbon Capture, Utilization, and Storage Experts' Workshop. September 26-28, 2017, Houston, U.S.A. Available at: https://www.energy.gov/sites/default/files/2018/05/f51/Accelerating%20Breakthrough%20Innovation%20in%20Carbon%20Capture%2C%20Utilization%2C%20and%20Storage%20_0.pdf. Accessed 8 May 2022.
2. Mission Innovation, Report of the Mission Innovation Carbon Capture, Utilization and Storage Experts' Workshop. June 19–20, 2019, Trondheim, Norway. Available at: http://mission-innovation.net/wp-content/uploads/2019/11/CCUS-Mission-Innovation-Challenge-Workshop-Report-Trondheim-2019.pdf. Accessed 8 May 2022.
3. National Petroleum Council, "CO_2 use" in *Meeting the Dual Challenge A Roadmap to At-Scale Deployment of Carbon Capture, Use, and Storage* (National Petroleum Council, Washington, 2019), chap. 9.
4. A. Dindi, D. V. Quang, L. F. Vega, E. Nashef, M. R. M. Abu-Zahra, Applications of fly ash for CO_2 capture, utilization, and storage. *J. CO2 Util.* **29**, 82–102 (2019).
5. Global CCS Institute, Global status of CCS: CCS accelerating to net zero (2021). Available at: https://www.globalccsinstitute.com/wp-content/uploads/2021/10/2021-Global-Status-of-CCS-Report_Global_CCS_Institute.pdf. Accessed 8 May 2022.
6. W. Seifritz, CO_2 disposal by means of silicates. *Nature* **345**, 486 (1990).
7. T. Tomkinson, M. R. Lee, D. F. Mark, C. L. Smith, Sequestration of Martian CO_2 by mineral carbonation. *Nat. Commun.* **4**, 2662 (2013).
8. J. M. Matter, P. B. Kelemen, Permanent storage of carbon dioxide in geological reservoirs by mineral carbonation. *Nat. Geosci.* **2**, 837–841 (2009).
9. P. Renforth, C. L. Washbourne, J. Taylder, D. A. C. Manning, Silicate production and availability for mineral carbonation. *Environ. Sci. Technol.* **45**, 2035–2041 (2011).
10. D. Daval, Carbon dioxide sequestration through silicate degradation and carbon mineralisation: Promises and uncertainties. npj Mater. *Degrad.* **2**, 11 (2018).
11. F. Xi *et al.*, Substantial global carbon uptake by cement carbonation. *Nat. Geosci.* **9**, 880–883 (2016).
12. I. M. Power *et al.*, Carbon mineralization: From natural analogues to engineered systems. *Rev. Mineral. Geochem.* **77**, 305–360 (2013).
13. D. J. Beerling *et al.*, Potential for large-scale CO_2 removal via enhanced rock weathering with croplands. *Nature* **583**, 242–248 (2020).
14. A. Sanna, M. Uibu, G. Caramanna, R. Kuusik, M. M. Maroto-Valer, A review of mineral carbonation technologies to sequester CO_2. *Chem. Soc. Rev.* **43**, 8049–8080 (2014).
15. F. Wang, D. B. Dreisinger, M. Jarvis, T. Hitchins, The technology of CO_2 sequestration by mineral carbonation: Current status and future prospects. *Can. Metall. Q.* **57**, 46–58 (2018).
16. N. R. Galina, G. L. A. F. Arce, I. Ávila, Evolution of carbon capture and storage by mineral carbonation: Data analysis and relevance of the theme. *Miner. Eng.* **142**, 105879 (2019).
17. A. Azdarpour *et al.*, Carbon dioxide mineral carbonation through ph-swing process: A review. *Energy Procedia* **61**, 2783–2786 (2014).
18. G. L. Arce, T. G. Soares Neto, I. Ávila, C. M. Luna, J. A. Carvalho, Leaching optimization of mining wastes with lizardite and brucite contents for use in indirect mineral carbonation through the pH swing method. *J. Clean. Prod.* **141**, 1324–1336 (2017).
19. A. Hemmati *et al.*, Solid products characterization in a multi-step mineralization process. *Chem. Eng. J.* **252**, 210–219 (2014).
20. S. Y. Pan *et al.*, CO_2 mineralization and utilization by alkaline solid wastes for potential carbon reduction. *Nat. Sustain.* **3**, 399–405 (2020).
21. H. Xie *et al.*, Enhancement of electricity generation in CO_2 mineralization cell by using sodium sulfate as the reaction medium. *Appl. Energy* **195**, 991–999 (2017).
22. J. Wang, K. Nakamura, N. Watanabe, A. Okamoto, T. Komai, $NaHCO_3$-promoted olivine weathering with H_2 generation and CO_2 sequestration in alkaline hydrothermal system. *IOP Conf. Ser.: Earth Environ. Sci.* **257**, 012017.
23. Y. Zhang, R. Wang, Z. Liu, Z. Zhang, A novel carbonate binder from waste hydrated cement paste for utilization of CO_2. *J. CO2 Util.* **32**, 276–280 (2019).
24. S. Stopic *et al.*, Synthesis of nanosilica via olivine mineral carbonation under high pressure in an autoclave. *Metals (Basel)* **9**, 708 (2019).
25. F. M. Baena-Moreno *et al.*, Converting CO_2 from biogas and $MgCl_2$ residues into valuable magnesium carbonate: A novel strategy for renewable energy production. *Energy* **180**, 457–464 (2019).
26. J. L. Hamilton *et al.*, Fate of transition metals during passive carbonation of ultramafic mine tailings via air capture with potential for metal resource recovery. *Int. J. Greenh. Gas Control* **71**, 155–167 (2018).
27. J. L. Hamilton *et al.*, Accelerating mineral carbonation in ultramafic mine tailings via direct CO_2 reaction and heap leaching with potential for base metal enrichment and recovery. *Econ. Geol.* **115**, 303–323 (2020).
28. W. K. O'Connor *et al.*, "Final report: Aqueous mineral carbonation: Mineral availability, pretreatment, reaction parametrics and process studies" (Tech. Rep. DOEARC-TR-04-002, Department of Energy, 2005).
29. W. J. J. Huijgen, R. N. J. Comans, G. J. Witkamp, Cost evaluation of CO_2 sequestration by aqueous mineral carbonation. *Energy Convers. Manage.* **48**, 1923–1935 (2007).

30. F. Wang, D. Dreisinger, M. Jarvis, T. Hitchins, L. Trytten, CO_2 mineralization and concurrent utilization for nickel conversion from nickel silicates to nickel sulfides. *Chem. Eng. J.* **406**, 126761 (2021).
31. Nickel, Trading Economics. Available at: https://tradingeconomics.com/commodity/nickel. Accessed 18 April 2022.
32. K. Kashefi, A. Pardakhti, M. Shafiepour, A. Hemmati, Process optimization for integrated mineralization of carbon dioxide and metal recovery of red mud. *J. Environ. Chem. Eng.* **8**, 103638 (2020).
33. L. C. Zappala, R. D. Balucan, J. Vaughan, K. M. Steel, Development of a nickel extraction-mineral carbonation process: Analysis of leaching mechanisms using regenerated acid. *Hydrometallurgy* **197**, 105482 (2020).
34. F. Wang, D. Dreisinger, M. Jarvis, T. Hitchins, Kinetics and mechanism of mineral carbonation of olivine for CO_2 sequestration. *Miner. Eng.* **131**, 185–197 (2019).
35. D. Sandalow *et al.*, *Carbon Mineralization Roadmap* (ICEF Innovation Roadmap Project, November 2021). https://www.icef.go.jp/pdf/summary/roadmap/icef2021_roadmap.pdf. Accessed 8 May 2022.
36. National Academies of Sciences, Engineering, and Medicine, *Negative Emissions Technologies and Reliable Sequestration: A Research Agenda* (National Academies of Sciences, Engineering, and Medicine, Washington, DC, 2019).
37. P. Renforth, The negative emission potential of alkaline materials. *Nat. Commun.* **10**, 1401 (2019).
38. T. Watari *et al.*, Total material requirement for the global energy transition to 2050: A focus on transport and electricity. *Resour. Conserv. Recycling* **148**, 91–103 (2019).
39. F. Wang, D. Dreisinger, M. Jarvis, T. Hitchins, Kinetic evaluation of mineral carbonation of natural silicate samples. *Chem. Eng. J.* **404**, 126522 (2021).
40. F. Wang, D. Dreisinger, M. Jarvis, T. Hitchins, D. Dyson, Quantifying kinetics of mineralization of carbon dioxide by olivine under moderate conditions. *Chem. Eng. J.* **360**, 452–463 (2019).
41. R. Santos *et al.*, Nickel extraction from olivine: Effect of carbonation pre-treatment. *Metals (Basel)* **5**, 1620–1644 (2015).
42. Q. R. S. Miller *et al.*, Tunable manipulation of mineral carbonation kinetics in nanoscale water films via citrate additives. *Environ. Sci. Technol.* **52**, 7138–7148 (2018).
43. J. J. Eksteen, E. A. Oraby, V. Nguyen, Leaching and ion exchange based recovery of nickel and cobalt from a low grade, serpentine-rich sulfide ore using an alkaline glycine lixiviant system. *Miner. Eng.* **145**, 106073 (2020).
44. A. J. Francis, C. J. Dodge, J. B. Gillow, Biodegradation of metal citrate complexes and implications for toxic-metal mobility. *Nature* **356**, 140 (1992).
45. N. C. Li, A. Lindenbaum, J. M. White, Some metal complexes of citric and tricarballylic acids. *J. Inorg. Nucl. Chem.* **12**, 122–128 (1959).
46. A. Miličević, G. Branica, N. Raos, Irving-Williams order in the framework of connectivity index $^3\chi v$ enables simultaneous prediction of stability constants of bivalent transition metal complexes. *Molecules* **16**, 1103–1112 (2011).
47. A. E. Martell, R. M. Smith, *Critical Stability Constants* (Plenum Press, New York, 1974), vol. 1, pp. 204–211.
48. A. E. Lewis, Review of metal sulphide precipitation. *Hydrometallurgy* **104**, 222–234 (2010).
49. R. R. Sheha, A. H. Harb, I. E. T. El-sayed, H. H. Someda, Removal of ethylenediaminetetraacetic acid and its cobalt complex by layered double hydroxide/titanium dioxide from aqueous solution. *Desalination Water Treat.* **57**, 16466–16472 (2016).
50. J. Chen, J. Gao, X. Wang, Thermal decomposition of ethylenediaminetetraacetic acid in the presence of 1,2-phenylenediamine and hydrochloric acid. *J. Braz. Chem. Soc.* **17**, 880–885 (2006).
51. G. Gadikota, J. Matter, P. Kelemen, A.-H. A. Park, Chemical and morphological changes during olivine carbonation for CO_2 storage in the presence of NaCl and $NaHCO_3$. *Phys. Chem. Chem. Phys.* **16**, 4679–4693 (2014).